ISSN 2176-5480

22nd International Congress of Mechanical Engineering (COBEM 2013)
November 3-7, 2013, Ribeirão Preto, SP, Brazil

EVALUATION OF AIR FLOW AND PARTICLE DEPOSITION IN HUMAN LUNG FOR THREE BREATHING CONDITIONS USING COMPUTATIONAL FLUID DYNAMICS (CFD)

Liliana de Luca Xavier Augusto*
Christian Carlos Cândido da Silva
José Antônio Silveira Gonçalves
Federal University of São Carlos (UFSCar) – Department of Chemical Engineering – São Carlos, São Paulo, Brazil.
liliana.lxa@gmail.com*; christianc.candido@gmail.com; jasgon@ufscar.br

Abstract. *The deposition of 10 µm particles in a triple airway bifurcation was investigated by numerical simulation. For this, Computational Fluid Dynamics (CFD) were used to solve transport equations for steady, laminar and isothermal flow; then, by the velocity field, the path of the particles was obtained, by the action of gravitational force and inertial impaction. Three breathing conditions were considered to represent resting, moderate and heavy activities (15, 30 and 60 L/min, at the trachea). The deposition on the airway internal surfaces was calculated and compared to experimental data to validate the model. The results showed that more particles were collected on the walls in the first bifurcation because of the inertial impaction and that the deposition increase with the respiratory activity. Thus, the air flow and particle deposition could be represented by CFD model used in this work and can be used for better understanding of deposition pattern of drugs or dust particles. It could be concluded that CFD can be applied for analysis in medicine field, without the high costs and time involved in experimental tests.*

Keywords: *Human airways bifurcations, Particle deposition, Computational Fluid Dynamics (CFD).*

1. INTRODUCTION

The air flow and particle deposition studies have applications in medicine and air quality fields. According to World Health Organization (WHO), the chronic inhalation of particulate matter may be the cause of respiratory diseases such as carcinoma, emphysema, silicosis and also cardiovascular diseases. It is important to know the deposition patterns in the human lugs to manage these diseases, by the utilization of inhalers and bronchodilators using by asthma and bronchitis patients, for example. Thus, the capability to evaluate where the deposition is more intense, known as hot spots, can assist in the development of inhalers and nebulizers, to ensure that the drug medicine particles reach the desirable region affected by the disease.

WHO also states that the air pollution is the main risk to the health, and the urban outdoor pollution is the cause of 1.3 million deaths per year, while indoor pollution is the main responsible for 2 million premature deaths in developing countries. Almost half of the indoor pollution victims are children under 5 years old.

Computational Fluid Dynamics (CFD) is a tool capable to provide velocity, pressure and temperature fields of flows, as well mass transfer between phases, using numerical simulation, without the high costs and time associated to experimental studies. Therefore, CFD is an alternative to the improvement of projects and researches. In some works, the determination of the deposition patterns is performed by *in vivo* experiments, as presented in the works of Bennett (1991) and Möller et al. (2009). One method used to get the images in these cases is through inhalation of radioactive air and aerosols, which permit to know the locals where the particles were deposited on the lung internal surfaces. However, this procedure can cause many health problems to the individuals involved in the tests. Considering this, CFD can be an alternative in the studies of particle deposition, because it does not use *in vivo* experiments to obtain the results and it does not offer risk to the health. Besides, CFD allows the analysis of the system response under different conditions and changing the variables that affects the flow.

The purpose of this work is to study the air flow and the deposition of microparticles in a triple airway bifurcation model in three different breathing conditions (resting, moderate and intense activity) using CFD.

2. METHOD

2.1 Model and Mesh Construction

A three-dimensional triple airway bifurcation was built, corresponding to third to sixth generations according to Weibel (1963) convention, using the software ANSYS-Design Modeler 14.0®, as shown in Fig. 1. Weibel (1963) considered that all generations are numbered to facilitate their localization and trachea is represented by number 0.

ISSN 2176-5480

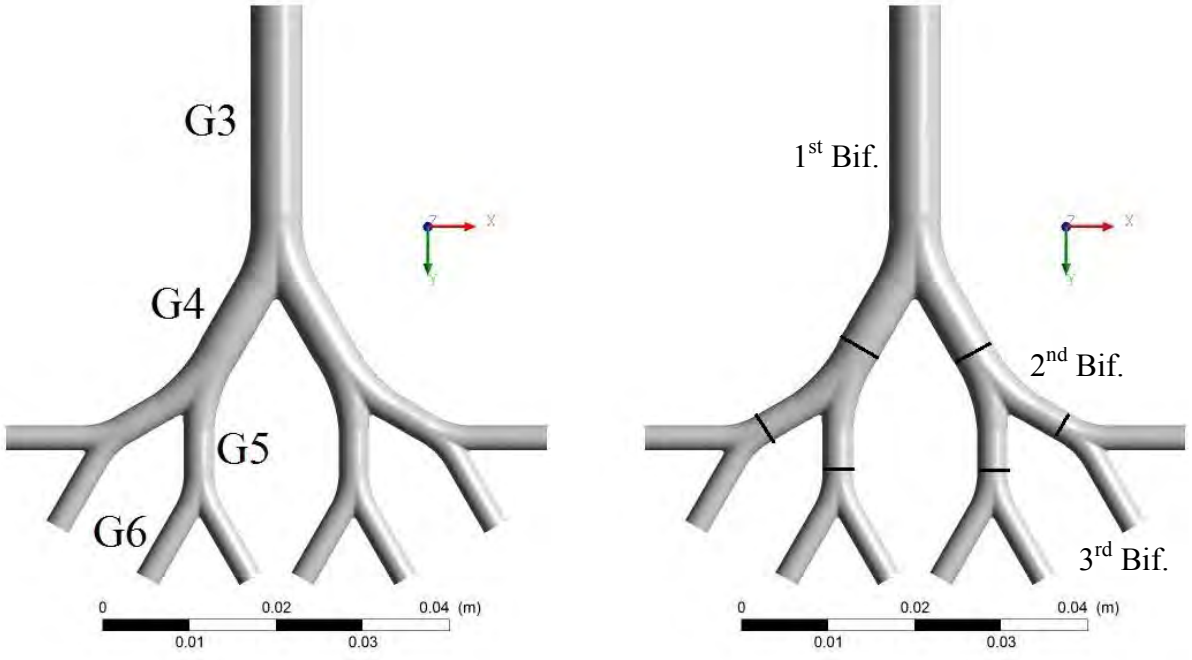

Figure 1. Four generations (G3-G6) and three bifurcations model.

In Tab. 1, the geometric parameters used by Zhang et al. (2002) are presented. They have been used in this work due to the similarity to those adopted in the studies of Kim and Fisher (1999), which was used to validate the model proposed here.

Table 1. Geometric parameters (adapted from Zhang et al. (2002)).

Generation	Diameter ($m/10^3$)	Length ($m/10^3$)
G3	6	24
G4	5	8.36
G5	3.5	4.37
G6	2.9	9.28

For the simulation, the symmetry condition in plane YZ and x=0 was considered, since the geometry and physical phenomena are symmetric with respect to YZ plane. Furthermore, tests were performed using complete and symmetric geometries, and they showed that the velocity profiles and deposition efficiencies (DE) were very close, confirming that this consideration is reasonable.

After build the geometry, it was divided in many finite volumes in which the governing equations were solved. The hexahedral mesh was generated using the software ANSYS-ICEM CFD 14.0®. To determine the total number of elements, the mesh was refined until the velocity fields and deposition efficiency remain almost constant. The grid independence evaluation led to 305,158 elements and 321,564 nodes. Near to the wall, the mesh was refined if compared to the rest of the computational domain, to capture with more accuracy all phenomena that govern the particle deposition on the wall. Figure 2 presents some mesh details, like symmetric 3rd generation and the outlet of 6th generations.

ISSN 2176-5480

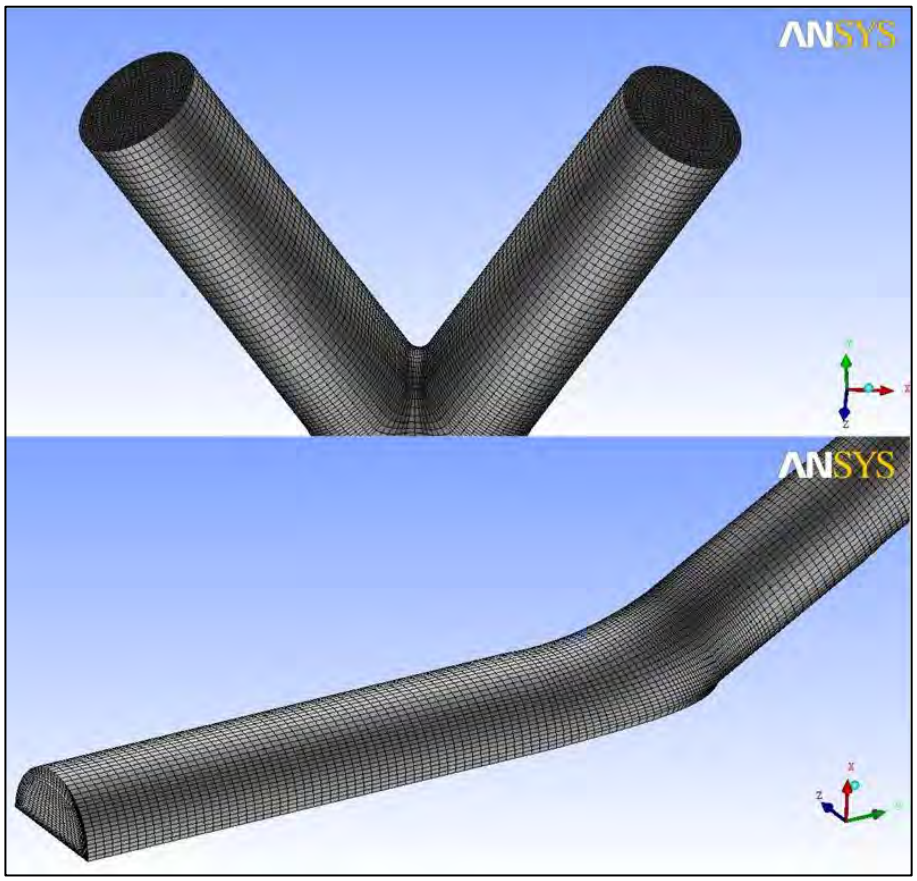

Figure 2. Details of finite volume mesh.

2.2 Governing Equations

To obtain the velocity fields, the continuity, Eq. (1), and momentum, Eq. (2), were solved to steady-state, incompressible, laminar and isothermal at 310.15 K flow.

$$\frac{\partial \rho}{\partial t} + \nabla \cdot (\rho \boldsymbol{v}) = 0 \tag{1}$$

$$\frac{\partial (\rho \boldsymbol{v})}{\partial \boldsymbol{t}} + \nabla \cdot (\rho \boldsymbol{v} \otimes \boldsymbol{v}) = \nabla \cdot p + \nabla \cdot \left[\mu \left(\nabla \boldsymbol{v} + \left(\nabla \boldsymbol{v}^{\boldsymbol{T}}\right)\right)\right] + \rho \boldsymbol{g} \tag{2}$$

where ρ is the air density (1.123 kg/m³), **v** is the fluid velocity vector, **g** is the gravity (9.81 m/s²), p is the pressure and μ is the fluid dynamic viscosity (1.90×10^{-5} Pa s).

Because the dispersed phase is diluted, it was considered that the particles don't influence fluid flow and the one-way coupled method was chosen for the simulations. Using Eulerian-Lagrangian approach for fluid and particle, respectively, the trajectory of the particle can be estimated by the Eq. (3):

$$m_p \frac{d^2 x_p}{dt^2} = \frac{1}{8} \pi \rho \frac{C_D}{C_{slip}} d_p^2 (\boldsymbol{v} - \boldsymbol{v}_p) |\boldsymbol{v} - \boldsymbol{v}_p| + m_p \boldsymbol{g} \tag{3}$$

where $\mathbf{x}_p$, m_p, d_p, $\mathbf{v_p}$ is the displacement, mass, diameter and velocity vector of the particle, respectively, and **g** is the gravity vector, C_D is the drag coefficient, and C_{slip} is the slip correction factor (or Cunningham correction factor). C_D and C_{slip} are given as:

$$C_D = \frac{24}{\mathrm{Re}_p} \left(1 + 0.15\, \mathrm{Re}_p^{0.687}\right), \; for \; \mathrm{Re}_p < 800 \tag{4}$$

ISSN 2176-5480

$$C_{slip} = 1 + Kn\left(2.514 + 0.8\exp\left(\frac{0.55}{Kn}\right)\right) \tag{5}$$

where Re_p is the particle Reynolds number, given by Eq. (6), and Kn is the Knudsen number, given as the ratio of the mean free path (Eq. (7)) to the particle diameter. For Re_p higher than 800, a value of 0.45 for the drag force coefficient can be used, according to Crowe et al. (2012).

$$Re_p = \frac{\rho\left|\mathbf{v} - \mathbf{v_p}\right| d_p}{\mu} \tag{6}$$

$$\lambda = \frac{2.15\times 10^{-4}\,\mu T^{1/2}}{p} \tag{7}$$

where μ is the dynamic fluid viscosity, T is the absolute temperature in K and p is the pressure in bar.

As presented above, the forces acting on the particles were drag and gravitational forces. Brownian motion can be disregarded, once that mechanism is more effective on small particles such as submicron or nanoparticles. Beyond that, considering that particles are not rotating and not interact among themselves, lift forces can be also disregarded.

To define the inlet velocity, three breathing conditions were considered (15, 30 and 60 L/min) to represent resting, moderate and heavy activities, respectively. Since these are the velocities at the trachea, the values were divided by a factor of 8, because the airways bifurcate three times until reach G3 (the inlet of the computational domain used in this work). At the inlet of the domain, a parabolic velocity profile was used for the fluid and for the 20,000 particles released. This inlet velocity was chosen to represent a fully-developed profile since turbulence only occurs in the trachea and firsts bifurcations. According to Xi et al. (2008), turbulent effects are negligible as from third generation. For the outlets at G6, a uniform static pressure was assigned. All the particles that collide with the wall surfaces deposit immediately due to the moist and spongy aspect of the airway surfaces. For this, parallel and perpendicular restitution coefficients of the wall were set to zero in the wall boundary condition.

2.3 Numerical Method

The software ANSYS-CFX 14.0® was used to solve all the governing equations stated previously. A subroutine in Fortran was written to insert Eq. (4), Eq. (5), Eq. (6), Eq. (7) into CFX 14.0 code. CFX algorithm solves the equations numerically using the element-based finite volume method, which involves the integration of the governing equations in nodes of all control volume of the computational domain, the discretization of the resulting equations in a algebraic equations system and, for solve this system, it uses a iterative method to find the final solution. In this work, the solutions are assumed converged when the dimensional residuals are smaller than 10^{-5}.

3. RESULTS

3.1 Model Validation

The model has been validated with experimental data provided by Kim and Fisher (1999). The authors used glass tubes to mimic a double airway bifurcation and tagged oil particles with uranine. The deposition efficiencies for each bifurcation were plotted by Stokes number (Eq. (8)) and a curve was fitted, in the form of Eq. (9).

$$St = \frac{\rho_p d_p^2 \bar{v}}{18\,\mu d} \tag{8}$$

$$\%DE = 100\left[1 - \frac{1}{aSt^{\,b} + 1}\right] \tag{9}$$

where St is the Stokes Number, $\bar{v}$ is the mean flow velocity in the parent tube, d is the diameter of the tube, a and b are constants.

The comparison between experimental data and results of simulation was performed considering that deposition efficiency only depends on Stokes number. Kim and Fisher (1999) provided data of deposition efficiencies for first and second bifurcations separately. Therefore, the fitted curves of both experimental and simulated data are shown in Fig. 3 and Fig. 4, for first and second bifurcations, respectively.

ISSN 2176-5480

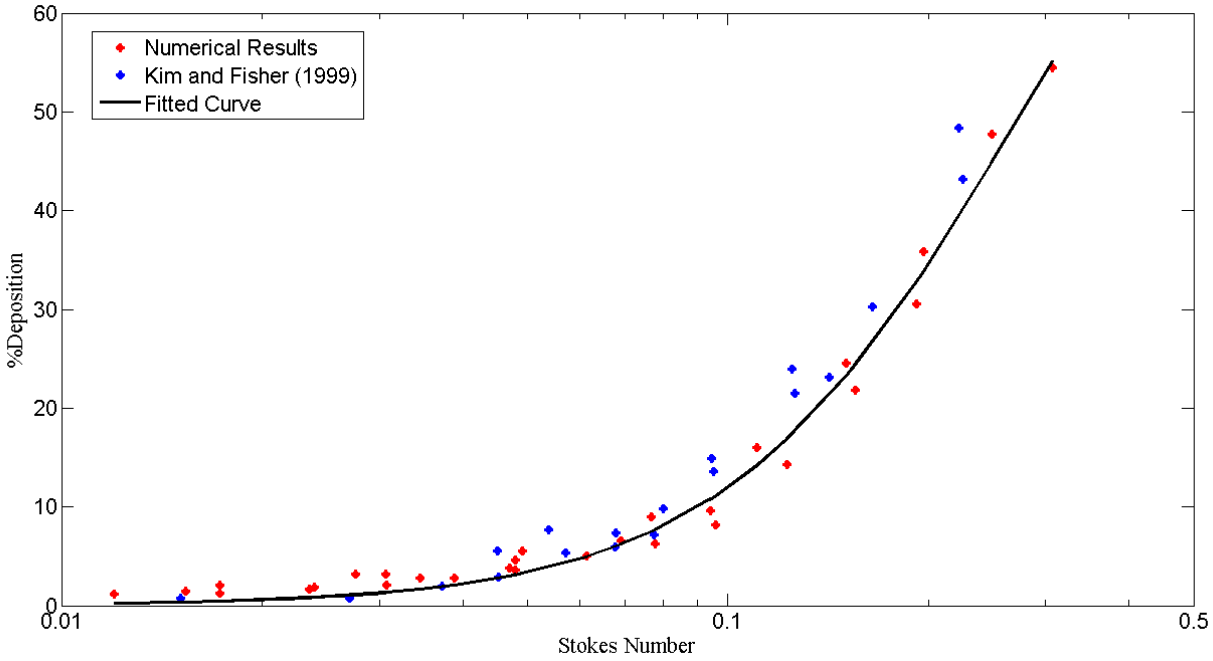

Figure 3. Comparison between experimental and simulated deposition efficiency for first bifurcation.

In Fig.3, results of simulated and experimental tests are shown. The curve was adjusted by the least square method ($R^2 = 0.997$) according to the simulated data symbolized by red points.

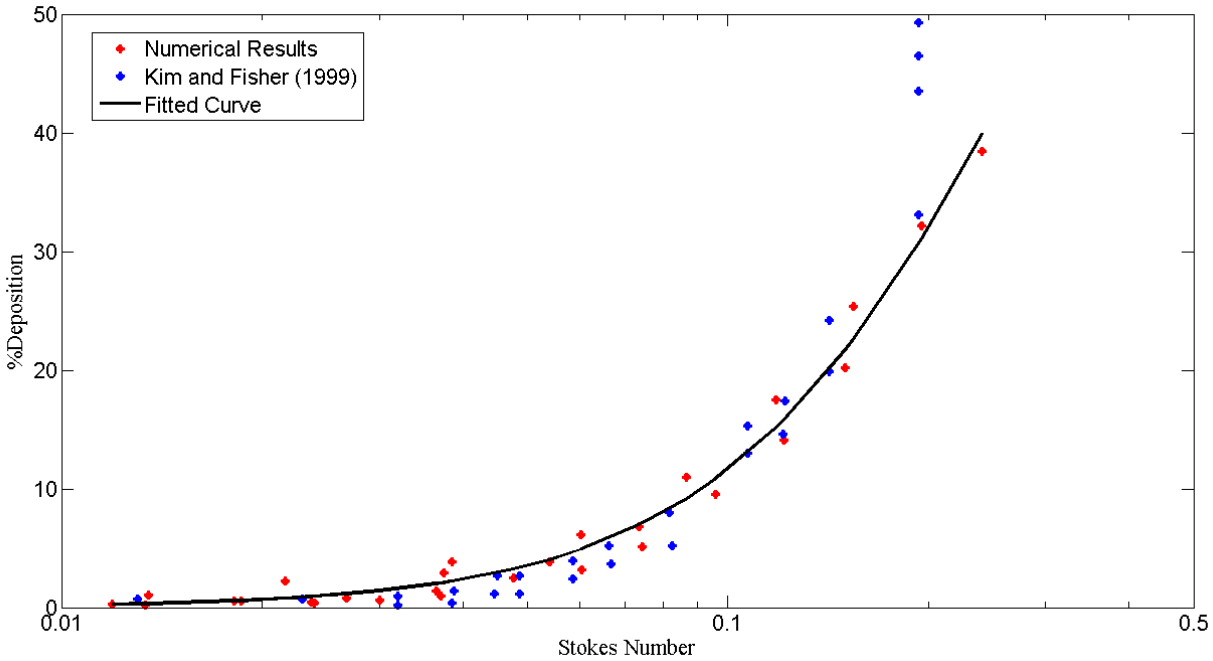

Figure 4. Comparison between experimental and simulated deposition efficiency for second bifurcation.

Experimental and simulated data are shown in Figure 4, in which the red curve was fitted using the least square method (R^2=0.992), using the red points.

In summary, good agreements between experimental and simulated results have been achieved and thus the model considered in this work could accurately predict the deposition of particles in a triple airway bifurcation.

ISSN 2176-5480

3.2 Air Flow Fields

The air flow fields are presented in Fig. 5 for the three breathing levels (resting, moderate and heavy activities) from XY plane. It can be observed that the profile was similar for the three cases, differing only by velocity magnitude. The parabolic velocity profile at the inlet makes the flow more intense in the inner generations. In fourth generation, the flow is divided, while in the fifths generations the reconstruction of a parabolic profile starts again and continues to form in sixths ones.

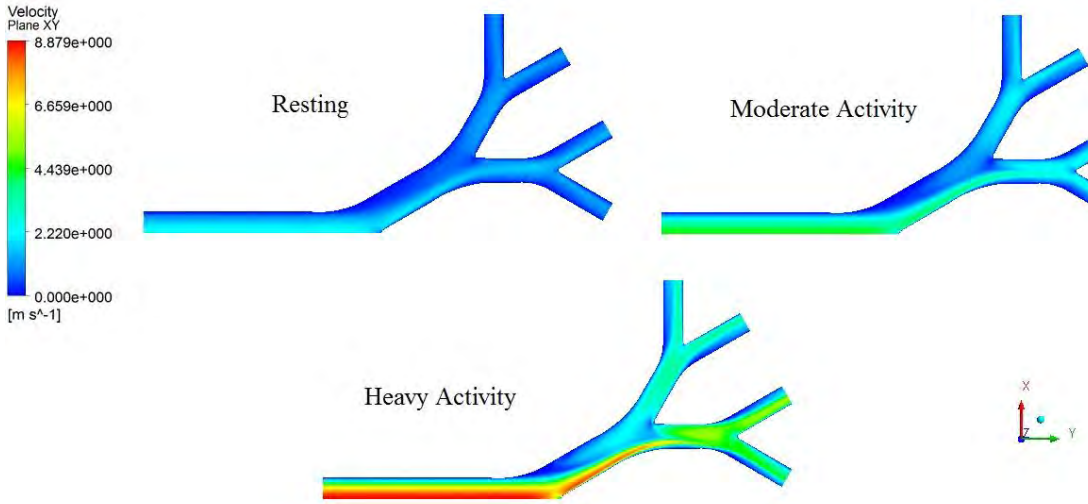

Figure 5. Flow fields in plane XY for three breathing levels.

Secondary velocities are shown in Fig. 6 for forth and fifths generations, for resting level. Cross-sectional axial velocities for third and fifths generations are not presented here, because the flow is almost fully-developed and results in a parabolic profile. According to Dean and Hurst (1927), secondary motion is produced by a given pressure gradient where the primary motion is the greatest and lead to outward movement.

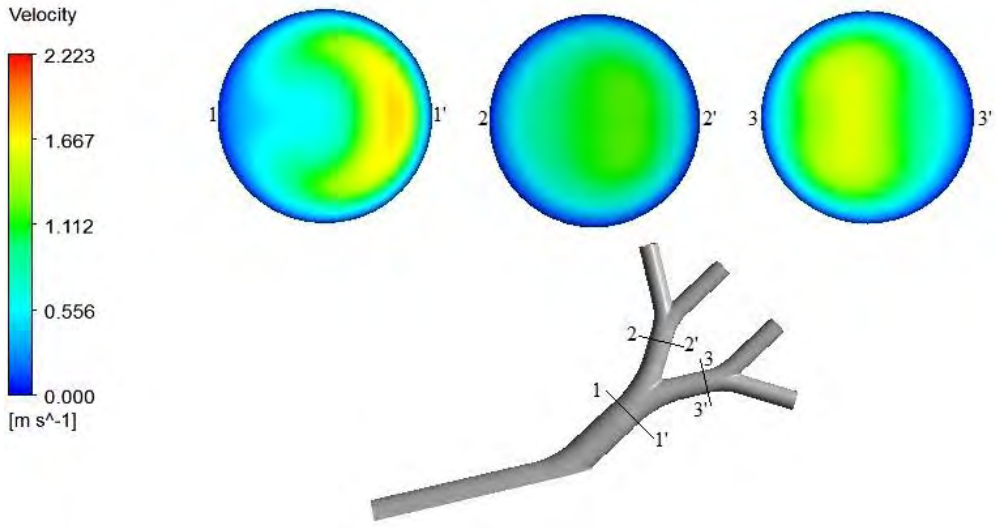

Figure 6. Secondary velocity distributions for resting.

Figure 6 confirms that air flow is more intense near inner walls, a common characteristic of flow in bifurcated ducts. Because of this, the particles are directed toward airway surfaces. Furthermore, it can be observed that vortical motions are beginning to act in the fourth generations due to fluid inertia which prevents the streamlines to follow the curvatures. In the fifths generations, the fluid inertia is less important and, so, the vortical motions are less pronounced.

ISSN 2176-5480

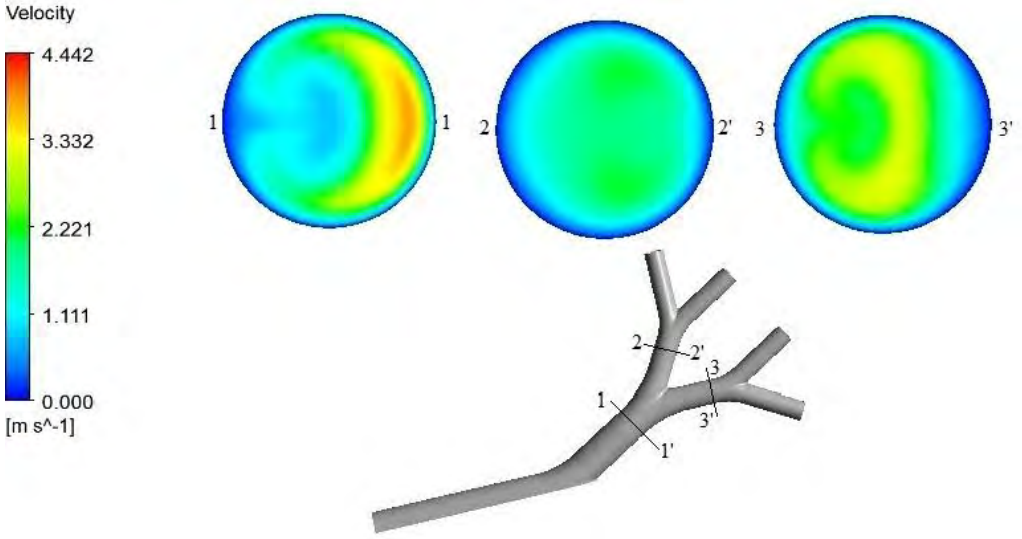

Figure 7. Secondary velocity distributions for moderate activity.

In Fig. 7, the secondary velocity distributions are presented for moderate activity. The behavior is similar to that shown in Fig. 6. However, the rotating vortices are more pronounced due to higher inertia, resulted from the increase of velocity at the inlet. The increase in secondary motion may be the reason for more particles deposit at the airway walls for moderate activity, if compared to resting condition.

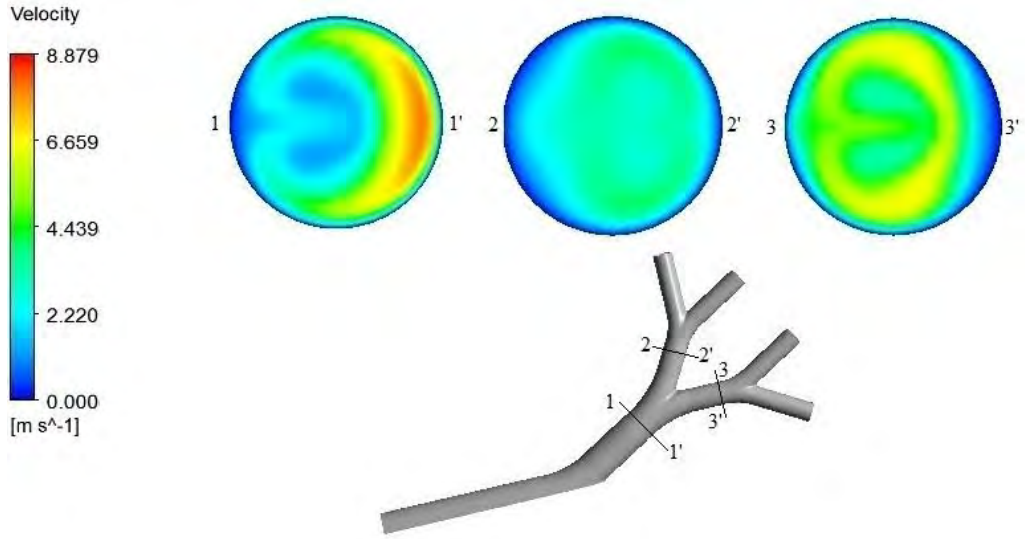

Figure 8. Secondary velocity distributions for heavy activity.

For heavy activity (Fig. 8), the flow follows the trend to raise the vortical motion. In this case, the inertia is higher enough to create rotating vortices that increase significantly the deposition efficiency over airway surfaces significantly if compared to the others breathing conditions.

As observed above, the vortical motion increases with the velocity. This kind of flow makes more particles deposit on the wall airway surfaces due higher inertia. Similar results were found by Zhang et al. (2002), Longest and Vinchurkar (2008) and Piglione et al. (2012).

3.3 Particle Deposition

The particle deposition in airway bifurcations can be estimated by two different ways. The branch-averaged deposition efficiency (DE) is defined as the ratio of particles deposited in a bifurcation by the number of particles that entered that bifurcation. DE was used above for validated the model used in this work. The deposition fraction (DF) can be calculated by the number of particles deposited in a bifurcation by the total number that entered the domain. Thus, the DF of the total geometry can be estimated by the sum of individuals DFs for each bifurcation.

ISSN 2176-5480

The deposition of 10 µm particles with 2,000 kg/m³ density was investigated under three breathing conditions, considering drag and gravitational forces acting on them. Below, deposition fraction is presented for resting, moderate and heavy activities, for each bifurcation, in Fig. 9 and Fig. 10.

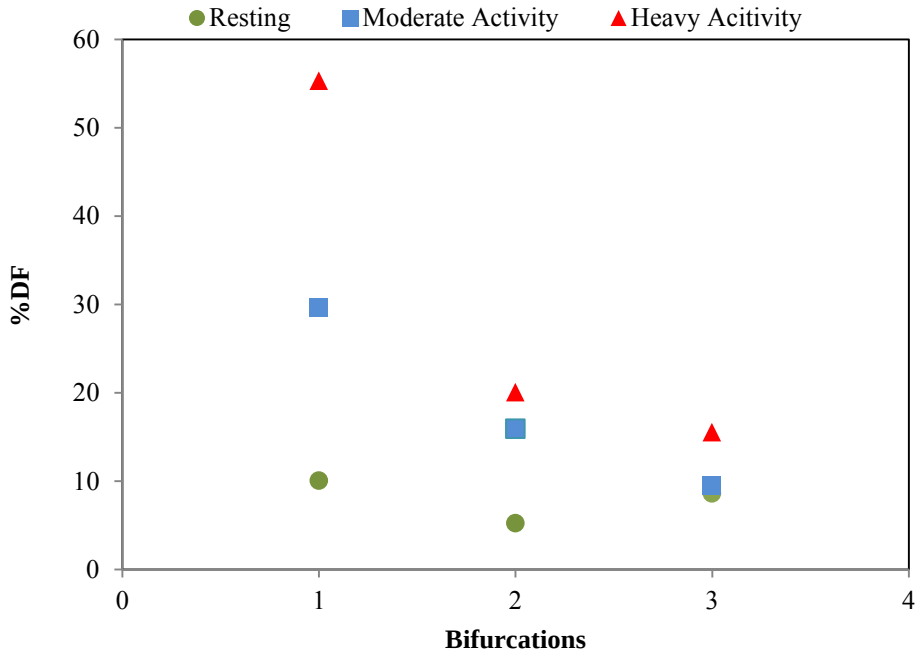

Figure 9. Deposition fraction for three bifurcations.

Figure 9 shows a higher deposition in the first bifurcation for all the three cases. It can be observed that the deposition was higher for the first bifurcation, for all breathing conditions, due to the drag force on the particles that makes them do not follow the streamlines in curved regions. Furthermore, the particle is relatively large if compared to nanoparticles, increasing the deposition by inertial impaction.

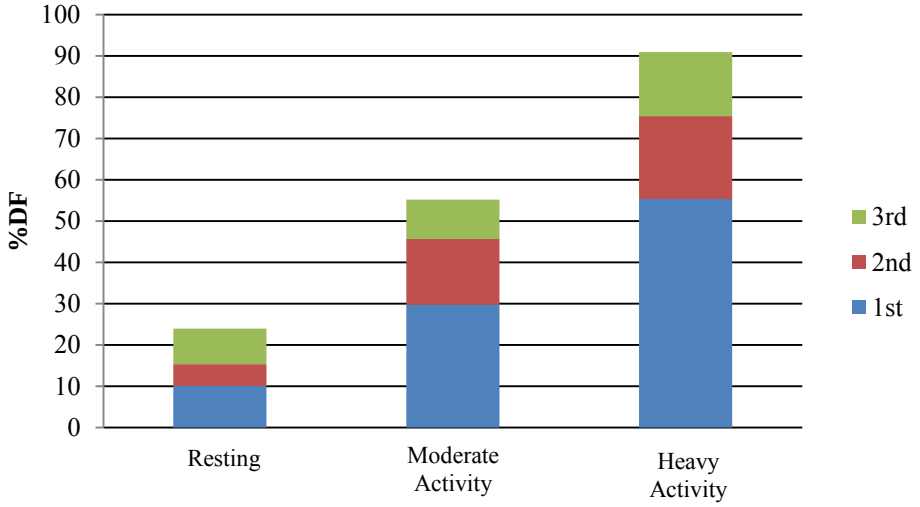

Figure 10. Cumulate fraction deposition for three breathing conditions.

Analyzing the Fig. 10, it can be inferred that an increase in the intensity of the activity, the total deposition also increase significantly, as expected. It can be observed that the deposition efficiency increases with the values of Reynolds and Stokes numbers due to the higher velocities and more intense vortical motion. Similar results were found for deposition pattern by Zhang et al. (2002) and Saber and Heydari (2012).

ISSN 2176-5480

4. CONCLUSIONS

The proposal of this work was evaluate the deposition and compare three breathing conditions for 10 μm particles in airway bifurcations based on Weibel (1963) model. Experimental and simulated data were compared and presented good agreement. The results showed that the deposition increases as the flow increases (from resting to heavy activity). Furthermore, more particles deposit in first bifurcation due inertial impaction which makes the particles leave the fluid streamlines and hit on the wall surfaces. This evidenced CFD as an alternative to estimate the deposition in biological systems, which are difficult to reach experimentally, and could be used to improve inhalable devices for drug aerosols and to understand the effect the dust particles deposited about respiratory diseases.

5. ACKNOWLEDGEMENTS

The authors would like to thank the Conselho Nacional de Desenvolvimento Científico e Tecnológico (CNPq) for providing the master's scholarship.

6. REFERENCES

Bennet, W. D., 1991. "Targeting Respiratory Drug Delivery with Aerosols Boluses". *Journal of Aerosol Medicine*, v. 4, n. 2, p. 69-78.

Crowe, C. T.; Schwarzkopf, J. D.; Sommerfeld, M.; Tsuji, Y., 2012. *Multiphase Flows With Droplets and Particles*. CRC Press, New York, 2nd edition.

Dean, W. R., Hurst, J. M., 1927. "Note of the Motion of Fluid in a Curved Pipe". *Philosophical Magazine*, v. 4, n. 7, p. 77-85.

Kim, C. S.; Fisher, D. M., 1999. "Deposition Characteristics of Aerosol Particles in Sequentially Bifurcating Airway Models". *Aerosol Science and Technology*, v. 31, n. 2-3, p. 198-220.

Longest, P. W.; Vinchurkar, S., 2008. "Inertial Deposition of Aerosols in Bifurcating Models During Steady Expiratory Flow". *Journal of Aerosol Science*, v. 40, n. 4, p. 370-378.

Möller, W.; Meyer, G.; Scheuch, G.; Kreyling, W. G.; Bennet, W. D., 2009. "Left-to-Right Asymmetry of Aerosol Deposition after Shallow Bolus Inhalation Depends on Lung Ventilation". Journal of Aerosol Medicine and Pulmonary Drug Delivery, v. 22, n. 4, p. 333-339.

Piglione, M. C.; Fontana, D. Vanni, M., 2012. "Simulation of Particle Deposition in Human Central Airways". *European Journal of Mechanics B/Fluids*, v. 31, p. 91-101.

Saber, E. M.; Heydari, G., 2012. "Flow Patters and Deposition Fraction on Particles in Range 0.1-10 μm at Trachea and the First Third Generations Under Different Breathing Conditions". *Computers in Biology and Medicine*, v. 42, n. 5, p. 631-638.

Weibel, E. R., 1963. *Morphometry of the Human Lung*. Academic Press, New York, 1st edition.

World Health Organization, 2011. Media Centre: Air Quality and Health Factsheet n. 313. 30 May, 2013 <http://www.who.int/mediacentre/factsheets/fs313/en/index.html>.

Xi, J.; Longest, P. W.; Martonen, T. B., 2008. "Effects of the Laryngeal Jet on Nano- and Microparticle Transport and Deposition in an Approximate Model of the Upper Tracheobronchial Airways". *Journal of Applied Physiology*, v 104, n. 6, p. 1761-1777.

Zhang, Z.; Kleinstreuer, C.; Kim, C. S., 2002. "Gas-Solid Two-Phase Flow in a Triple Bifurcation Lung Airway Model". *International Journal of Multiphase Flow*, v. 28, n. 6, p. 1021-1046.

7. RESPONSIBILITY NOTICE

The authors are the only responsible for the printed material included in this paper.